

## Synthesis of New Red-Emitting Single-Phase Europium Oxycarbonate

Vilas G. Pol,<sup>\*,†</sup> Jose M. Calderon-Moreno,<sup>‡</sup> Monica Popa,<sup>‡</sup> Somobratra Acharya,<sup>§</sup> Katsuhiko Ariga,<sup>§</sup> and P. Thiyagarajan<sup>†,||</sup>

<sup>†</sup>IPNS, Argonne National Laboratory, Argonne, Illinois 60439, <sup>‡</sup>Institute of Physical Chemistry “Ilie Murgulescu”, Academia Romana, 202 Splaiul Independentei, 060021 Bucharest, Romania, <sup>§</sup>World Premier International (WPI) Research Center for Materials Nanoarchitectonics (MANA), National Institute for Materials Science (NIMS), 1-1 Namiki, Tsukuba, Ibaraki, 305-0044, Japan, and <sup>||</sup>Office of Basic Energy Sciences, Department of Energy, SC-22.1/Germantown Building, 1000 Independence Ave. SW, Washington, DC 20585

Received February 12, 2009

A fascinating one-pot solvent-, catalyst-, and template-free synthesis process to facilitate a single-phase crystalline hexagonal type-II luminescent  $\text{Eu}_2\text{O}_2\text{CO}_3$  organization comprised of nanoplates is demonstrated. The thermolysis (700 °C) of europium acetate in a closed stainless steel reactor under autogenic pressure [ $\sim 3$  MPa] yielded  $\text{Eu}_2\text{O}_2\text{CO}_3$  superstructures. Powder X-ray diffraction, high-resolution transmission electron microscopy, and Raman measurements confirmed the structure. Fourier transform infrared spectroscopy, energy-dispersive spectrometry, and CHNS analysis verified the composition. Scanning electron microscopy corroborated the morphology of the new  $\text{Eu}_2\text{O}_2\text{CO}_3$  compound, and the primary luminescence properties are accounted.

### Introduction

Europium oxide ( $\text{Eu}_2\text{O}_3$ ) is one of the most important oxide phosphors and has been widely applied in low-voltage cathodoluminescent devices, high-density optical storage devices, and lasers because the central emission band of  $\text{Eu}^{3+}$  is at about 612 nm, which is one of the three primary colors.<sup>1</sup> Previously, several  $\text{Eu}_2\text{O}_3$  nanostructures such as nanoparticles,<sup>2</sup> nanorods,<sup>3</sup> nanowires,<sup>4</sup> hollow spheres,<sup>5</sup> and nanotubes<sup>6</sup> have been prepared by different methods. Cui et al. reported the synthesis of luminescent europium methacrylate nanowires and their thermal conversion into  $\text{Eu}_2\text{O}_3$  nanotubes.<sup>7</sup> Additionally, rare earth oxycarbonates with the hexagonal type-II structure are also suitable for the host materials of phosphors. There are three types of crystal structures in rare earth oxycarbonates,  $\text{RE}_2\text{O}_2\text{CO}_3$  (RE = rare earths), that is, tetragonal type I, monoclinic type Ia, and hexagonal type II.<sup>8</sup> Among these three structures, the type-II

oxycarbonate is the most stable one and has a high chemical stability against water and carbon dioxide.<sup>9</sup>

However, it is difficult to obtain single-phase hexagonal type-II oxycarbonates; thus, very few studies on their complicated preparation and characterization have been reported. For example,  $\text{La}_2\text{O}_2\text{CO}_3$ -II was prepared by the carbonation of  $\text{La}_2\text{O}_3$  under a stream of carbon dioxide at 850 °C for 5 days, and  $\text{Nd}_2\text{O}_2\text{CO}_3$ -II was synthesized by the decomposition of neodymium acetate hydrate at 500 °C and subsequent firing for 5 more days at 765 °C under flowing carbon dioxide.<sup>10</sup>  $\text{Gd}_2\text{O}_2\text{CO}_3$ -II is obtained as a single phase by annealing the carbonate for several weeks in a stream of  $\text{CO}_2$ .<sup>8</sup> Recently, Masui et al. employed alkaline metal carbonates as the flux to promote the formation of oxycarbonates of  $\text{La}_2\text{O}_2\text{CO}_3$ -II<sup>11</sup> and  $\text{Gd}_2\text{O}_2\text{CO}_3$ -II<sup>12</sup> in a single phase by heating the precursors in a flow of 10%  $\text{CO}_2$ /90%  $\text{N}_2$  gas for 12 h at atmospheric pressure. Dysprosium oxycarbonates were prepared in the type-II phase form by the hydrothermal treatment of their carbonates at considerably high pressures of 1400–3400 atm.<sup>13</sup> However, to the best of our knowledge, single-phase  $\text{Eu}_2\text{O}_2\text{CO}_3$ -II has not yet been synthesized; evidently, luminescence studies are not carried out.

\*To whom correspondence should be addressed. E-mail: vilaspol@gmail.com.

- (1) Bezig, E.; Trautman, J. K. *Science* **1992**, *257*, 189.
- (2) Wakefield, G.; Keron, H. A.; Dobson, P. J.; Hutchison, J. L. *Adv. Mater.* **1999**, *215*, 179.
- (3) Pol, V. G.; Palchik, O.; Gedanken, A.; Felner, I. *J. Phys. Chem. B* **2002**, *106*, 9737.
- (4) Wong, K.-L.; Law, G.-L.; Murphy, M. B.; Tanner, P. A.; Wong, W.-T.; Lam, P. K.-S.; Hon-Wah, L. M. *Inorg. Chem.* **2008**, *47*, 5190.
- (5) Zhang, L.; Luo, J.; Wu, M.; Jiu, H.; Chen, Q. W. *Mater. Lett.* **2007**, *61*, 4452.
- (6) Yang, H.; Zhang, D.; Shi, L.; Fang, J. *Acta Materialia* **2008**, *56*, 955.
- (7) Cui, F.; Zhang, J.; Cui, T.; Liang, S.; Ming, L.; Gao, Z.; Yang, B. *Nanotechnology* **2008**, *19*, 65607.
- (8) Turcotte, R. P.; Sawyer, J. O.; Eyring, L. *Inorg. Chem.* **1969**, *8*, 238.

- (9) Imanaka, N.; Kamikawa, M.; Adachi, G. *Anal. Chem.* **2002**, *74*, 4800.
- (10) Olafsen, A.; Larsson, A.-K.; Fjellva, H.; Hauback, B. C. *J. Solid State Chem.* **2001**, *158*, 14.
- (11) Tamura, S.; Koyabu, K.; Masui, T.; Imanaka, N. *Chem. Lett.* **2004**, *33*, 58.
- (12) Masui, T.; Mayama, Y.; Koyabu, K.; Imanaka, N. *Chem. Lett.* **2005**, *34*, 1236–1237.
- (13) Crystensen, A. N. *Acta Chem. Scand.* **1973**, *27*, 1835.

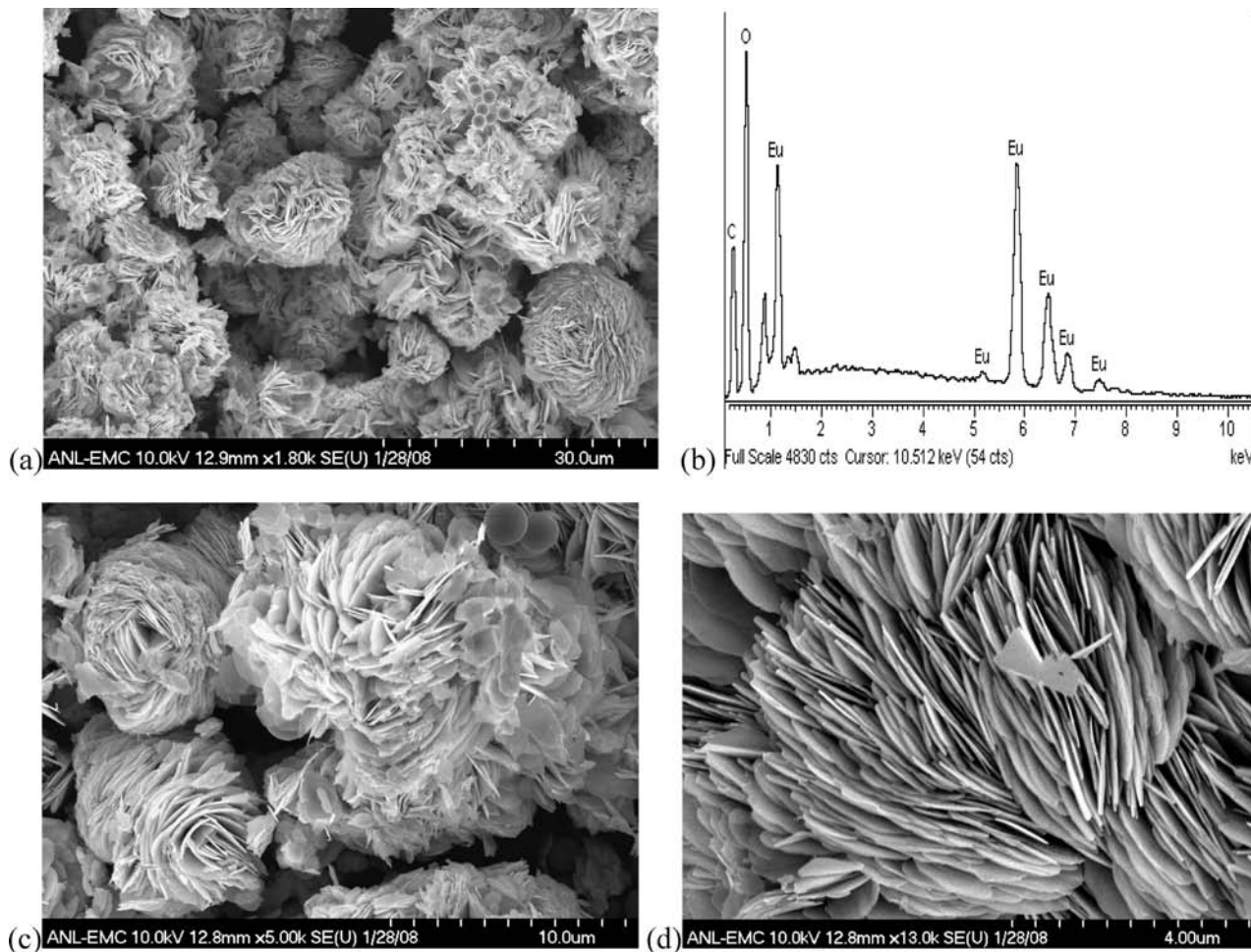


**Figure 1.** (a) SEM image of as-prepared EOC, (b) EDS of EOC, (c) HR-SEM of an individual EOC, and (d) parallel stacking of nanoplates within EOC.

This paper demonstrates a one-pot, solvent-, catalyst-, and template-free; efficient synthesis process to prepare single-phase  $\text{Eu}_2\text{O}_2\text{CO}_3$  europium oxycarbonate (EOC) luminescent plates. The thermolysis of a europium acetate (EA) precursor in a closed stainless steel (SS) reactor at 700 °C under *autogenic* pressure [ $\sim 3$  MPa] yielded  $\text{Eu}_2\text{O}_2\text{CO}_3$  plates. We have systematically characterized as-prepared EOCs to determine their morphology (scanning electron microscopy, SEM), structure (X-ray diffraction, XRD; Raman spectroscopy; high-resolution transmission electron microscopy, HR-TEM), and composition (energy dispersive X-ray, EDX; Fourier transform infrared spectroscopy, FT-IR). This is the earliest report on the single-phase synthesis of crystalline hexagonal type-II  $\text{Eu}_2\text{O}_2\text{CO}_3$  plates followed by photoluminescence (PL) studies.

### Experimental Section

Europium acetate [EA,  $\text{Eu}(\text{O}_2\text{C}_2\text{H}_3)_3$ ] was purchased from Sigma-Aldrich and used as received. In a typical synthesis of EOC roses, 1 g of EA was introduced in a 5 mL SS reactor at room temperature in an inert nitrogen atmosphere. The 1/2 in.-diameter SS union part is initially sealed at one end using a cap. The partially filled SS reactor with EA was closed tightly with the other cap in an inert nitrogen environment and placed at the center of a box furnace for uniform heating. The temperature of the furnace was ramped up to 700 °C at a rate of 40 °C/min and maintained at that temperature for various times. The maximum pressure of  $\sim 3$  MPa is measure

at 700 °C during EA dissociation. Upon naturally cooling the SS reactor to room temperature, we obtained 0.54 g of gray powder, which was directly characterized for its morphological, compositional, structural, and PL properties.

The phase purity and crystal structure of the EOC were determined using XRD and Raman spectroscopy. The XRD pattern was recorded by using a Bruker AXSD\* Advance powder X-ray diffractometer (Cu  $K\alpha$  radiation, wavelength 1.5406 Å). The Raman spectrum was recorded at room temperature by using a triple Jobin Yvon/Atago-Bussan T-6400 spectrometer, equipped with an  $\text{Ar}^+$  laser ( $\lambda = 514.5$  nm) and a liquid- $\text{N}_2$  cooled CCD detector. The morphology of the thin films was observed by SEM and an EDX-equipped SEM instrument. The IR spectrum of EOC was obtained at a resolution of  $2\text{ cm}^{-1}$ , over the frequency range from 4000 to  $400\text{ cm}^{-1}$ , using a model Perkin-Elmer spectrophotometer. The spectrum was taken from thin ( $\sim 20\text{ mg/cm}^2$ ) KBr pellets containing samples of approximately 1 wt %. Pellets were prepared by compacting an intimate mixture obtained by grinding 1 mg of the substance in 100 mg of KBr powder.

### Results and Discussion

The thermal decomposition of EA at 700 °C for 3 h in a closed SS reactor converted the micrometer-size EA particles to europium oxycarbonate plates. The SEM image in Figure 1a clearly demonstrates the captivating organization of hundreds of EOC nanoplates. The original micrometer-size

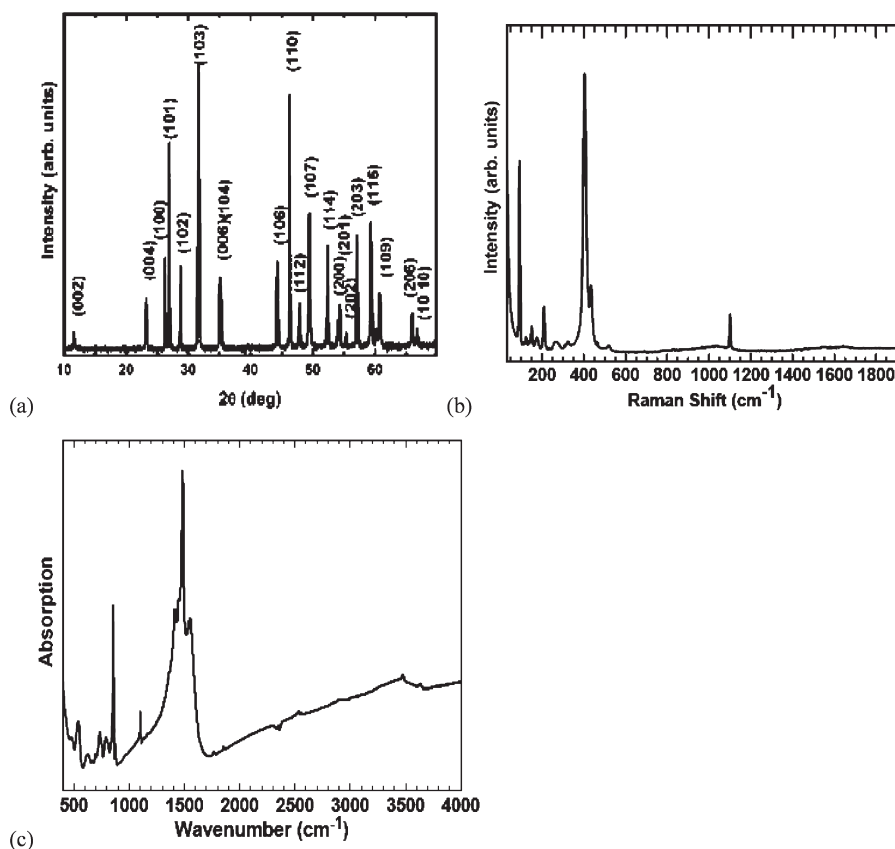


**Figure 2.** (a) The XRD pattern, (b) Raman spectrum, and (c) IR spectrum of the EOC sample.

EA particles are consumed to grow upward to fabricate superstructures under critical experimental conditions. The EDX spectrum (Figure 1b) of EOC detected Eu, O, and C as the major elements and small amounts of an Al signal (non assigned) arising from sample holder without additional impurities. The calculated element percentages of Eu, O, C, and H in the EA precursor are 46.2, 29.2, 21.9, and 2.7%, respectively. The C, H, and N analysis of EOC verified the elemental amounts of C, H, and N as  $4.8 \pm 0.5$ ,  $< 0.5$ ,  $< 0.5$  wt %, respectively. Considering the product formula  $\text{Eu}_2\text{O}_2\text{CO}_3$ , the calculated amounts of the Eu, C, and O are 76.76, 3.03, and 20.2 wt %, respectively. It means that some excess amount of carbon is left over in the EOC product. That formed completely spherical 2–3- $\mu\text{m}$ -diameter carbon particles, as observed in the SEM (Figure 1a and in c). The significant lessening in the amounts of C and H are noticed and might have produced hydrocarbons at 700 °C, which promoted the conversion of EA to EOC. The HR-SEM image (Figure 1c) further depicts that individual  $\text{Eu}_2\text{O}_2\text{CO}_3$  structures have 10–15  $\mu\text{m}$  outer diameters. Figure 1d exhibits the parallel stacking of EOC nanoplates, which are grown upward with close packing. The diameters of the plates are  $\sim 35$  nm, while the widths are at several micrometers. The reaction time of 1 or 2 h initiated the growth process but, however, was insufficient for complete growth. More than 3 h of reaction time did not show any morphological difference in the appearance of the formed morphology.

The crystalline structure of the EOC was identified by XRD using Cu K $\alpha$  radiation. The pattern corresponds to a hexagonal type-II polymorph of europium oxycarbonate (space group  $P63/mmc$ ) and is in good agreement with other isostructural oxycarbonates, that is,  $\text{Gd}_2\text{O}_2\text{CO}_3$ ,<sup>12</sup>

$\text{Sm}_2\text{O}_2\text{CO}_3$ ,  $\text{Y}_2\text{O}_2\text{CO}_3$ ,<sup>14</sup> and  $\text{La}_2\text{O}_2\text{CO}_3$ .<sup>15</sup> The single-phase oxycarbonate (Figure 2a) was obtained without any impurity peaks in the diffraction pattern. The unit cell parameters of the hexagonal  $\text{Eu}_2\text{O}_2\text{CO}_3$  are  $a = 0.3920$  nm and  $c = 1.535$  nm, respectively. This report demonstrates the superficial synthesis of single-phase crystalline  $\text{Eu}_2\text{O}_2\text{CO}_3$ . An XRD coherent crystalline domain size of  $\sim 30$  nm was calculated from the 004, 103, and 110 reflections using Scherrer's method, which matches with SEM measurements. The XRD measurements have demonstrated that the single-phase hexagonal type-II  $\text{Eu}_2\text{O}_2\text{CO}_3$  can be synthesized using the present straightforward synthetic approach. In order to confirm the absence of secondary or grain boundary phases, detailed micro-Raman spectroscopy measurements on EOC were carried out. The Raman spectrum of the hexagonal polymorph of EOC in Figure 2b shows a sharp band at  $92\text{ cm}^{-1}$ ; a stronger and broader feature at  $402\text{ cm}^{-1}$ ; and other less intense peaks at 124, 150, 176, 209, 266, 323, 434, 519, and  $1085\text{ cm}^{-1}$ . The band at  $1085\text{ cm}^{-1}$  corresponds to the vibrations of the carbonate group. The Raman spectra of rare earth sesquioxides exhibit a characteristic strong feature around  $350\text{ cm}^{-1}$  ( $\sim 340$  for  $\text{Eu}_2\text{O}_3$ )<sup>16–18</sup> which is not observed in our Raman measurements. Therefore, from both the Raman and XRD evidence,

(14) Imanaka, N.; Masui, T.; Mayama, Y.; Koyabu, K. *J. Solid State Chem.* **2005**, *178*, 3601.

(15) Koyabu, K.; Masui, T.; Tamura, S.; Imanaka, N. *J. Alloys Compd.* **2006**, *408*, 867.

(16) Dilawar, N.; Mehrotra, S.; Varandani, D.; Kumaraswamy, B. V.; Haldar, S. K.; Bandyopadhyay, A. K. *Mater. Characterization* **2008**, *59*, 462.

(17) Calderon-Moreno, J. M.; Yoshimura, M. *Solid State Ionics* **2002**, *154*, 125.

(18) Moreno, J. M. C. *Key Eng. Mater.* **2004**, *264–268*, 1373.

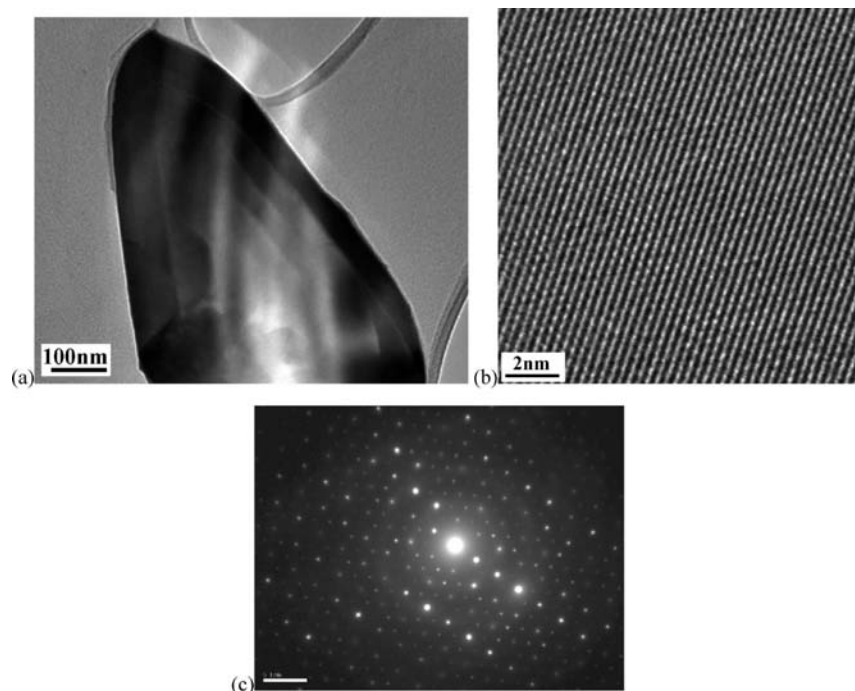


**Figure 3.** (a) TEM images of a single plate of EOC, (b) HR-TEM of EOC nanoplates, and (c) ED on EOC nanoplate.

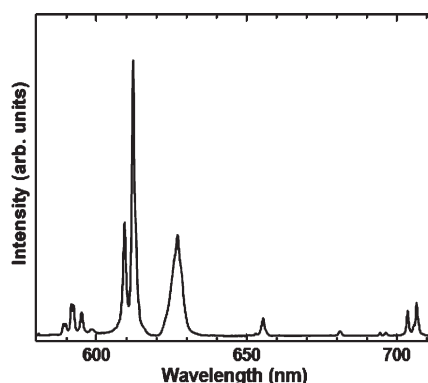


**Figure 4.** Photoluminescence spectrum of EOC sample.

we can exclude the formation of  $\text{Eu}_2\text{O}_3$ , and all the observed bands are attributed to single-phase  $\text{Eu}_2\text{O}_2\text{CO}_3$ .

The IR spectrum of the hexagonal  $\text{Eu}_2\text{O}_2\text{CO}_3$  (Figure 2c) shows bands at 1550, 1480, 1415, 1100, 855, 790, 740, 625, and  $540\text{ cm}^{-1}$ , similar to those reported for the single-phase samples of the hexagonal (type-II) rare earth oxycarbonates,<sup>8,9,19–22</sup> with characteristic peaks assignable to carbonate oxide species at 1480, 1415, 1100, 855, 790, and  $740\text{ cm}^{-1}$  due to vibration modes of  $\text{CO}_3^{2-}$ . The bands at 1480 and  $1415\text{ cm}^{-1}$  are attributed to the antisymmetric vibration bands ( $\nu_3$ ) of  $\text{CO}_3^{2-}$ , and the  $1100\text{ cm}^{-1}$  band corresponds to the symmetric vibration mode ( $\nu_1$ ). The bands at  $855\text{ cm}^{-1}$  are assigned to the  $\nu_2$  bending mode,<sup>20</sup> the out-of-plane bending region, and the weak bands at 740 and  $790\text{ cm}^{-1}$  are probably due to the  $\delta(\text{COO})^-$  deformation vibrations. The band at  $1550\text{ cm}^{-1}$  might be carboxylate groups, and the weak absorptions at

$625$  and  $540\text{ cm}^{-1}$  emerging at  $400\text{--}700\text{ cm}^{-1}$  can be related to Eu–O vibration modes.<sup>22</sup>

The TEM of EOC is presented in Figure 3a and demonstrates a single plate possessing sharp edges. The HR-TEM (Figure 3b) of the EOC nanoplates clearly shows lattice fringes with  $d_{101} = 3.331\text{ \AA}$  and provides evidence for the crystalline nature of the plates. The selected area electron diffraction is shown in Figure 3c, and the complex dot pattern obtained from various planes of EOC nanoplates also confirm high crystallinity.

The room-temperature PL spectrum obtained from EOC is displayed in Figure 4. Upon excitation at  $514\text{ nm}$ , the dominant narrow red emission at  $612\text{ nm}$  is observed. The emission bands correspond to the  $^5\text{D}_0 \rightarrow ^7\text{F}_J$  ( $J = 1, 2, 3, 4$ ) transitions of  $\text{Eu}^{3+}$  ions, which are mainly contributed by the localized rare earth 4f energy levels. The  $^5\text{D}_0 \rightarrow ^7\text{F}_1$  transition at  $590\text{ nm}$  was the parity-allowed magnetic dipole transition ( $\Delta J = 1$ ). The  $^5\text{D}_0 \rightarrow ^7\text{F}_2$  electric dipole transition at  $612\text{ nm}$  ( $\Delta J = 2$ ) was very sensitive to the local environment around the europium ion, and its intensity depended on the symmetry of the crystal field around the

(19) Goldsmith, J. A.; Ross, S. D. *Spectrochem. Acta A* **1967**, *23*, 1909.

(20) Popa, M.; Kakihana, M. *Solid State Ionics* **2001**, *141*, 265.

(21) Popa, M.; Kakihana, M. *J. Therm. Anal. Cal.* **2001**, *65*, 281.

(22) Hussein, G. A. M.; Buttrey, D. J.; DeSanto, P.; Abd-Elgaber, A. A.; Roshdy, H.; Myhoub, A. Y. Z. *Thermochim. Acta* **2003**, *402*, 27.

## Article

europium ion. A low symmetry around the europium ion increased the intensity of the electric dipole transition. Also, we could identify the emission bands at 654 and 710 nm, which originated from  $^5D_0 \rightarrow ^7F_3$  and  $^5D_0 \rightarrow ^7F_4$  transitions. Our EOC provided a pure red light emission, and the results clearly indicate that Eu atoms are stabilized in the  $3^+$  state in  $\text{Eu}_2\text{O}_2\text{CO}_3$ .

The obtained EOC sample exhibits good thermal stability, undergoing further thermal treatment for 3 h at 700 °C without morphological or structural changes, confirmed by SEM, XRD, Raman, TEM, and PL measurements. We believe that the nanoplates of EOC with hexagonal crystal structure are grown in a certain orientation under autogenic

pressure ( $\sim 3$  MPa) and formed during the dissociation of EA at 700 °C. Recently, comparable luminescent polar ZnO flowers consisting of ZnO nanopencils have been reported, where the zinc acetate was decomposed, employing analogous reaction conditions.<sup>23</sup> Since this is the foremost report on EOC synthesis, it is difficult to define an exact growth mechanism of EOC.

In summary, we have developed a solvent- and catalyst-free, one-pot synthesis process to fabricate a single-phase  $\text{Eu}_2\text{O}_2\text{CO}_3$  phosphor via thermolysis of a single precursor under autogenic pressure in a closed stainless steel reactor yielding luminescent structures comprised of 2D nanoplates. The systematic characterization of the as-prepared EOC determined the morphology, unique hexagonal type-II  $\text{Eu}_2\text{O}_2\text{CO}_3$  structure, composition, and photoluminescent properties.

(23) Pol, V. G.; Calderon-Moreno, J. M.; Thiyagarajan, P. *Langmuir* **2008**, *24*, 13640.